Evidence of light-emitting amorphous silicon clusters confined in a silicon oxide matrix

H. Rinnert, M. Vergnat, A. Burneau

Evidence of light-emitting amorphous silicon clusters confined in a silicon oxide matrix

H. Rinnert[a] and M. Vergnat
Laboratoire de Physique des Matériaux, (U.M.R. C.N.R.S. No 7556), Université Henri Poincaré Nancy 1, B.P. 239, 54506 Vandœuvre-lès-Nancy Cedex, France

A. Burneau
Laboratoire de Chimie Physique pour l'Environnement (U.M.R. C.N.R.S. No 7564), Université Henri Poincaré Nancy 1, 405, rue de Vandœuvre, 54506 Villers-lès-Nancy Cedex, France

(Received 18 May 2000; accepted for publication 9 October 2000)

Amorphous silicon oxide thin films were prepared by the coevaporation technique in ultrahigh vacuum. Different compositions were obtained by changing the evaporation rate of silicon. The samples were then annealed to different temperatures up to 950 °C. The composition and the structure were investigated using energy dispersive x-ray spectroscopy, infrared absorption measurements, and Raman spectroscopy. This study attests the presence of amorphous silicon clusters in a silicon oxide matrix. Optical transmission measurements were performed and interpreted in the field of the composite medium theory. The obtained results are in good agreement with the presented structural model. The photoluminescence in the red-orange domain was studied in relation with the structure. The correlation between the photoluminescence energy and intensity and the structure shows that the light emission originates from the silicon clusters embedded in the silicon oxide matrix. Moreover the dependence of the photoluminescence energy with the silicon volume fraction suggests the origin of the light emission could be due to a quantum confinement effect of carriers in the amorphous silicon clusters. © *2001 American Institute of Physics.*
[DOI: 10.1063/1.1330557]

I. INTRODUCTION

Since the observation of a strong visible photoluminescence (PL) at room temperature in porous silicon,[1] silicon-based light-emitting-materials are intensively studied. The usual way to obtain more efficient silicon-based optoelectronic devices is the preparation of materials with lower dimensions in which the carriers motion is reduced involving in an increase of the gap of the semiconductor and of the radiative recombination yield. A great number of techniques was used to obtain such structures and photoluminescence was observed in Si^+ implanted SiO_2 films,[2,3] in Si rich SiO_2 samples grown by chemical vapor deposition[4,5] or by sputtering[6] and in Si/SiO_2 multilayers.[7]

A very large range of PL wavelength was found from the ultraviolet to the near infrared domains. Although several explanations were proposed in which quantum confinement,[8,9] silicon-based chemical compounds,[10,11] interface states[12] or defects states[13] are implicated, the detailed origin of the PL is still matter in debate. It has been clearly shown that both porous silicon and silicon nanostructured films present two different PL bands.[14,15] While the first one, in the UV-blue-green domain, is generally attributed to radiative recombination from defect centers in the silicon oxide layer surrounding the silicon nanostructures,[16,17] the second one, in the red-orange domain, is generally attributed to the quantum confinement of carriers.[18,19] The PL evolution as a function of the silicon nanostructures size is a crucial test to assign, in silicon oxide thin films as well as in porous silicon, the PL origin to pure quantum confinement or to silicon oxide defects and/or interface states.

Theoretical works have shown that quantum confinement can appear for silicon structures with nanometer sizes in one, two, or three directions. The studied objects are mainly slabs, wires, and grains,[20–22] but the question of whether a crystalline structure is necessary or not to obtain PL is still an open question. Most of the published experimental results shed light on crystalline confined nanostructures and, for samples prepared in the amorphous state, the PL often appears after crystallization treatments.[23,24] Several theoretical works still propose that the crystallinity is not necessary to obtain the confinement effect and that amorphous silicon grains can allow radiative recombination in the visible range.[25,26]

In a previous work, we have shown that PL could be obtained in the visible range in pure and hydrogenated amorphous silicon oxide thin films prepared by the evaporation technique.[27] The observation of PL in unhydrogenated samples definitely rejects the role of hydrogenated silicon-based chemical species as a possible explanation of the PL. In the present work, the origin of the PL in the red-orange domain is studied in pure amorphous silicon oxide thin films. Evidence will be presented that the PL can be attributed to the carriers recombination in amorphous silicon clusters embedded in a silicon oxide matrix. A structural study is first presented to unambiguously show the existence of confined amorphous silicon nanostructures. The structural results are obtained from chemical analysis, electron diffraction, Raman

[a]Electronic mail: rinnert@lpm.u-nancy.fr

and infrared spectrometry, and optical measurements. PL experiments are performed and interpreted in relation with the composition and the structure of the films. The results presented here strongly support the assumption that the red-orange band emitted by confined silicon structures is attributed to a quantum confinement effect.

II. EXPERIMENT

The SiO_x alloys were prepared by the evaporation technique with a background pressure equal to 10^{-7} Torr onto substrates maintained at 100 °C. Four groups of samples were prepared to study the effect of the chemical composition. Group A was obtained by evaporation of SiO powder from a tantalum thermal cell. The groups B, C, and D were obtained by coevaporation of pure Si and SiO from an electron beam gun and the thermal cell, respectively. The deposition rate, equal to 0.1 nm s^{-1}, and the composition of the samples were controlled by a quartz microbalance system. By varying the deposition rates of Si and SiO, the samples were prepared with different stoichiometries. The average chemical composition x was analyzed by energy dispersive x-ray spectroscopy (EDXS). Each film was annealed at different temperatures T_a= 350, 500, 650, 800, and 950 °C in a quartz tube evacuated by an ionic pump. The background pressure was 10^{-7} Torr and the heating rate was equal to 10 K min^{-1}. The samples were cooled down immediately after the annealed temperature was reached. The samples were deposited onto different substrates. Silicon substrates were used for PL, Raman, IR measurements, and fused silica glass substrates were used for Raman and UV-Vis-NIR experiments. The thickness was 200 and 500 nm for silicon and glass substrates, respectively.

The oxygen bonding configurations were obtained from Fourier transform infrared transmission measurements using a Perkin-Elmer 2000 spectrometer with a resolution of 4 cm^{-1}. For each sample, a reference spectrum of an uncoated silicon substrate was subtracted from the experimental spectra. Raman and photoluminescence experiments were performed with a multichannel Jobin Yvon T64000 Raman spectrometer equipped with a charge coupled device camera cooled at 140 K. The excitation light source at 488 nm was emitted from a Spectra Physics argon laser with an incident power of around 10 mW/mm^2. Gratings with 1800 and 300 grooves/mm were used to disperse the reflected and emitted light for the Raman and photoluminescence experiments, respectively. Optical measurements were performed with a dispersive Varian Cary 5 spectrometer. Absorption spectra were obtained from 190 to 3000 nm, using two different light sources and two different detectors. An UV deuterium lamp and a wire tungsten lamp were used as sources, and a PbS photodetector and a photomultiplier as detectors. The substrates on which the films were deposited for the optical experiments were fused silica glasses so as to avoid absorption in the near UV and to avoid disturbance by the Si–O–H absorption in the near infrared range.

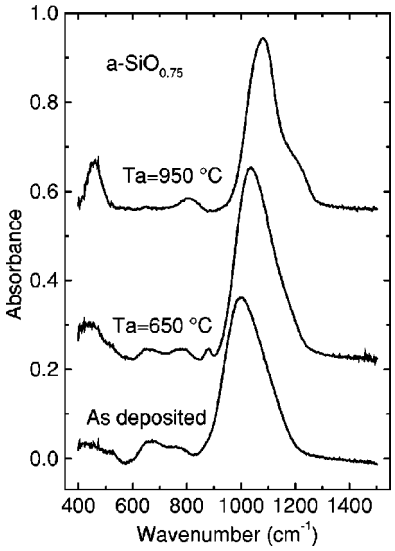

FIG. 1. Infrared absorption spectra of the samples of the group B for different annealing temperatures T_a.

III. RESULTS AND DISCUSSION

A. Chemical composition and structural characterization

1. Transmission electron microscopy and energy dispersive x-ray spectroscopy

Electron diffraction patterns showed that the films were amorphous whatever the annealing temperature. The non-crystallization of the film at high temperatures like 950 °C is not a surprising effect even if it is known that the crystallization temperature of amorphous silicon is equal to around 650 °C. Such results have already been obtained. Inokuma *et al.*[28] have shown, in the case of silicon suboxides prepared by cracking of silane, that the formation of crystallites appears for temperatures greater than 950 °C for a-$SiO_{1.65}$. Moreover Zacharias *et al.*[29] showed that the crystallization temperature, for Si/SiO_2 superlattices, increased rapidly with decreasing a-Si layer thickness. It seems that the crystallization is more difficult for small-dimensions clusters embedded in a dielectric matrix.

The energy dispersive EDXS technique allowed us to obtain the chemical composition of the samples. Five measurements were performed on each sample to determine the average composition of the SiO_x samples. The x value of the as-deposited samples is equal to 0.95, 0.75, 0.61, and 0.47 for samples A, B, C, and D, respectively. It was verified that the average composition was not modified by the annealing process. No further oxidation occurred either during exposure to air nor during annealing treatments.

2. Infrared absorption results

Infrared spectra are represented in Fig. 1 for the samples of group B at different annealing temperatures. For all samples, absorption bands at 450, 650, 800, and 1000 cm^{-1} are observed. With annealing treatments, the bands at 450 and 800 cm^{-1} increase while the band at 650 cm^{-1} decreases. The main absorption band shifts to the higher frequencies from 1000 cm^{-1} for the as-deposited sample to

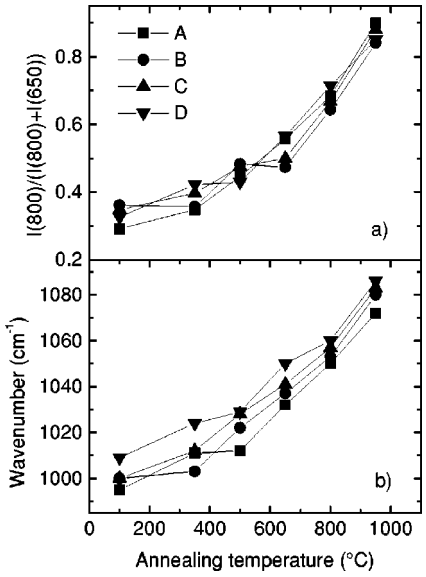

FIG. 2. Ratio $I(800)/(I(800)+I(650))$ and wave number of the asymmetric stretching vibration as a function of the annealing temperature T_a for the samples of groups A, B, C, and D.

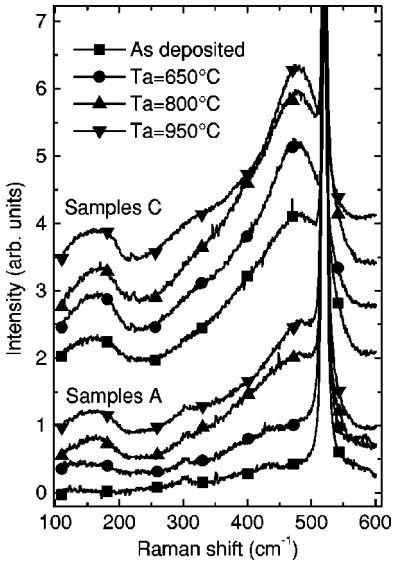

FIG. 3. Raman spectra of the samples of groups A and C for the different annealing temperatures T_a.

1080 cm^{-1} for T_a=950 °C. These bands are attributed to the infrared active vibrations of the Si–O–Si bonds. The vibration at 450 cm^{-1} is due to the rocking motion of this group. The absorption in the domain 650–800 and 1000 cm^{-1} is due to the symmetric and asymmetric stretching vibration of oxygen atom in the Si–O–Si group, respectively. These vibrations are present for all the SiO_x films but their frequencies are dependent on the environment of the Si atoms. Because of the strong electronegativity of the oxygen atom, these absorption frequencies are increasing functions of x. In the case of oxygen doped a-Si films and silicon dioxide films, these frequencies are equal to 450, 650, and 940 cm^{-1} [30–32] and 450, 800, and 1080 cm^{-1},[33,34] respectively. For the intermediate concentrations, a linear relation between x and the frequency of the asymmetric stretching vibration is generally accepted in an homogeneous silicon oxide film.[35–37]

The frequency of the Si–O–Si asymmetric stretching mode for a SiO film is nearly equal to 1000 cm^{-1}. The evolution with the annealing temperature observed in Fig. 1 suggests that the composition continuously evolved from SiO for the as-deposited film to SiO_2 for the film annealed at 950 °C. The oxidation degree of the film can be characterized by the position of the peak near 1000 cm^{-1}. As the peaks at 650 and 800 cm^{-1} correspond to the Si–O–Si symmetric stretching mode in silicon with low and high oxygen contents, respectively, the stoichiometry of the film can also be characterized by the ratio of $I(800)$ divided by $I(800)+I(650)$, where $I(800)$ and $I(650)$ are the integrated absorption of the 800 and 650 cm^{-1} peaks, respectively. This ratio and the frequency of the asymmetric stretching vibration are represented in Fig. 2 as a function of the annealing temperature for all the samples. The evolution of these values first shows that the evolution of the infrared spectra is independent of the initial composition of the films and that the suboxide has always evolved into silicon dioxide with annealing treatments. Moreover, as the average chemical composition determined by EDXS remains unchanged, it can be concluded that a phase separation appears in the film and that silicon rich areas appear in the samples.

3. Raman spectrometry

The Raman spectrometry is a very efficient technique to observe the presence and to study the structure of silicon clusters in the dielectric matrix. Crystalline silicon is characterized by a strong and thin band at 520.5 cm^{-1}, which corresponds to the transverse optic (TO) mode of phonons. In the case of amorphous silicon, the disorder induces changes in the vibrational density of states. The Raman spectrum is characterized by two large and weak bands at 150 and 480 cm^{-1} corresponding to transverse acoustic and transverse optic modes, respectively. Raman experiments were first performed for samples deposited on fused silica glass substrates. The absence of signal at 520.5 cm^{-1} means that all the samples are amorphous, which confirms the electron microscopy observations. As the substrates show a Raman band at 465 cm^{-1} which disturbs the spectra of the films in the domain of the TO mode of amorphous silicon, Raman experiments were then performed on silicon substrates. The spectra of the samples A and C are reported in Fig. 3 for different annealing temperatures. The strong peak at 520.5 cm^{-1} is the substrate signal. For the as-deposited sample A, no signal corresponding to pure amorphous silicon is detected. For as-deposited sample C, it is clear that a-Si domains are present in the film. This result means that the as-deposited coevaporated samples have silicon oxide and pure amorphous silicon domains. Whatever the chemical composition of the films, the bands at 150 and 480 cm^{-1} appear with the annealing treatments, which proves that pure a-Si clusters grow in the material. These results are in agreement with the EDXS and infrared spectrometry results. They strongly suggest that a phase separation process happens in the films to form the two more stable a-Si and a-SiO_2

phases. The structure modification could be due to a diffusion phenomenon of the oxygen atoms to form the SiO_2 stable phase. Such a phase separation has already been observed and studied and the reaction $2\times SiO_y \rightarrow y\times SiO_2 + (2-y)\times Si$ is proposed to explain the evolution of the structure.[38–40]

4. Determination of the silicon volume fraction

The structure of silicon suboxides and in particular of SiO is still a debating point. Two models are generally proposed to describe the structure. The random-bonding model (RBM) suggests that SiO can be considered as a homogeneous material where silicon and oxygen atoms are randomly dispersed. The mixture model (MM), on the contrary, maintains that the material is composed of pure silicon and pure silicon dioxide domains. Moreover, the structure of the material strongly depends on the preparation conditions and on the posttreatments. In the case of the as-deposited material A, the film is highly homogeneous and can be described by the RBM model. Indeed EDXS indicates an average composition equal to 0.95 and the frequency of the Si–O–Si asymmetric stretching vibration is the frequency generally attributed to the SiO stoichiometric phase. Furthermore, no *a*-Si domain is detected by the Raman experiments. The homogeneity of this sample is certainly due to the low substrate temperature that is too weak to allow a dissociation of the SiO groups coming from the evaporation source. For the coevaporated samples, the infrared spectrometry results show that the samples are inhomogeneous. Indeed the frequency of the Si–O–Si asymmetric stretching vibration is nearly the same as for sample A while the average chemical composition indicates a stronger concentration of silicon. These results suggest that the structure can be described by the mixture model. In the case of the annealed samples, the infrared results indicate a continuous oxidation of the samples with annealing, while EDXS has shown that the composition is unchanged. This proves that a phase separation process happened during annealing so as to form the thermodynamically stable phases *a*-Si and *a*-SiO_2. The appearance of the characteristic bands of *a*-Si in the Raman experiments confirms this interpretation.

Consequently the atomic structure of these films can be described by amorphous silicon clusters embedded in a SiO_y matrix. The estimation of the proportions of these two phases can be obtained from EDXS and infrared spectrometry results, which give the average composition and the stoichiometry y of the matrix, respectively. Indeed, the sample prepared by evaporation of SiO powder is homogeneous, as will be verified by Raman spectrometry. The value of the stoichiometry of the deposited film is 0.95 and the frequency of the IR absorption band is 995 cm^{-1}. When the film is annealed at high temperatures, the frequency becomes equal to 1080 cm^{-1}, the value corresponding to SiO_2 films. As proposed by Pai *et al.*,[35] we considered that there is a linear relation between the peak frequency ν of the Si–O infrared absorption band and the stoichiometry y of the silicon oxide phase. Hence, the relation $y=(\nu-918/81)$ was used. This formula gives the values 918 and 1080 cm^{-1} at the limits $x=0$ and $x=2$, which corresponds well to the values accepted for unhydrogenated films. Assuming that the densities of amorphous silicon and of amorphous silicon oxide are equal to 5×10^{22} and 6.6×10^{22} at./cm^3, respectively, the volume fractions v_{Si} and v_{SiO_y} of the different phases can be deduced. The values y and v_{Si} are represented in Fig. 4 as a function of the annealed temperature for the different compositions. Every as-deposited sample has a silicon oxide matrix with a stoichiometry near that of SiO and v_{Si} is an increasing function of the average silicon concentration. The effect of annealing is the same whatever the composition of the as-deposited material. Due to the phase separation, the pure silicon volume fraction increases continuously with the annealing temperature and for the annealed samples at 950 °C, the matrix is practically pure SiO_2.

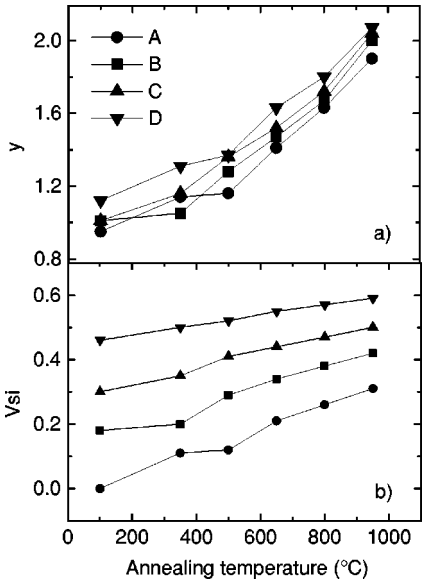

FIG. 4. Stoichiometry y of the silicon oxide phase and silicon volume fraction v_{Si} for the samples of groups A, B, C, and D.

B. Optical measurements

The study of the optical properties of *a*-SiO_x films, in particular of the refractive index n is a powerful way to investigate the structure of the material. The evolution of the refractive index with x is well known in the case of the homogeneous SiO_x silicon oxide films. n is a decreasing function of x, its value at 2.5 μm being equal to 4 for pure *a*-Si, to 2.3 for SiO and to 1.46 for *a*-SiO_2.[41] Other values were obtained for the whole range of x. The values of n evolve from 3.5 for low oxidized *a*-Si to 1.5 for *a*-SiO_2 for the samples obtained by Yeh *et al.*[42] and from 2.4 for *a*-$SiO_{0.1}$ to 1.46 for *a*-SiO_2 for the samples obtained by Haga *et al.*[43] The presence of silicon clusters in the films can strongly modify the refractive index of the silicon oxide film. If *a*-Si domains are present, the average chemical composition x is not the pertinent parameter for the evolution of the refractive index. n is dependent of y, namely the ratio of the number of oxygen atoms divided by the number of silicon atoms in the silicon oxide phase, but also of v_{Si}, namely the

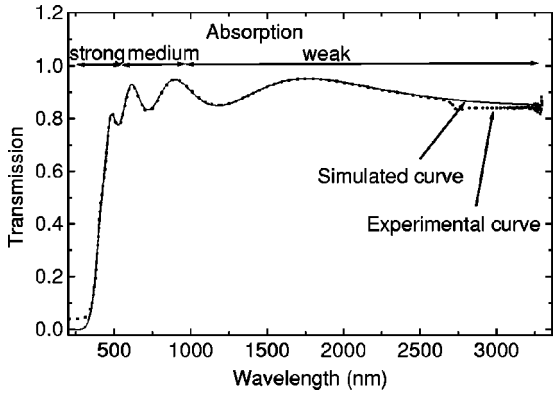

FIG. 5. Typical transmission spectrum in the Uv-Vis-Nir domain of a silicon oxide film. The dotted and solid lines are the experimental and simulated curves, respectively.

silicon volume fraction. The material must be seen as a composite material and n varies in agreement with the Lorentz theory.

In order to determine n, absorption measurements were performed for all samples as-deposited and annealed at different temperatures. A typical transmission spectrum is represented in Fig. 5. The interference phenomenon is due to the difference between the refractive indexes of the film and the substrate. In order to have strong interference fringes, the samples were prepared with a thickness equal to 500 nm. As in the case of amorphous silicon and amorphous silicon oxide, the transmission spectra (Fig. 5) can be decomposed in three domains: the strong absorption region, the medium absorption region, and the weak absorption region. In the strong absorption domain, the absorption coefficient α vary with a power law $\alpha E = B(E - E_g)^2$, where E_g is the optical gap, B a constant, and E the energy of the photon. In the medium absorption region α can be described by an exponential law. Finally in the weak absorption area, α is assumed to be negligible. As the absorption is very weak in the infrared region and as the interference fringes are clearly visible, the values n can be obtained with a very good precision by simulating the experimental spectra with the exact expression of the transmission taking into account of the interference phenomenon.[44] The variation with the wavelength λ of the refractive index of the fused silica substrate is known and the refractive index n of the film is simulated by a polynomial function of $1/\lambda$. The obtained values of n for $\lambda = 2.5\ \mu$m are given in Table I. The observation of these results clearly shows that the refractive index is correlated neither with x nor with y, but, if the film is considered as a composite material with the presence of pure a-Si and a-SiO_y domains, n is related to the refractive indexes n_{Si} and n_{SiO_y} of the pure a-Si phase and the pure a-SiO_y phase, respectively, by the Lorentz equation: $(n^2-1)/(n^2+2) = v_{Si}(n_{Si}^2-1)/(n_{Si}^2+2) + v_{SiO_y}(n_{SiO_y}^2-1)/(n_{SiO_y}^2+2)$. Assuming that n_{Si} is equal to 4, n_{SiO_y} can be deduced from this expression. The values of n_{SiO_y}, reported in Table I and represented in Fig. 6 as a function of y, show the correlation generally obtained in silicon oxide. That proves that the results of the optical experiments are in perfect agreement with our structural model which considers the films as a composite material with amorphous islands in a SiO_y matrix.

TABLE I. Experimental values of the refractive index n of the SiO_x films and calculated refractive index n_{SiO_y} of the SiO_y phase. y is the stoichiometry of the silicon oxide phase.

Samples group	T_a (°C)	y	n	n_{SiO_y}
A (x=0.95)	as-deposited	0.95	1.71	1.71
	350	1.14	1.69	1.61
	650	1.41	1.79	1.55
	800	1.63	1.83	1.52
	950	1.9	1.83	1.45
B (x=0.75)	as-deposited	1.01	1.92	1.72
	350	1.05	1.91	1.69
	650	1.47	1.98	1.56
	800	1.67	1.98	1.5
	950	2	1.99	1.44
C (x=0.61)	as-deposited	1.01	2.06	1.7
	350	1.16	2.03	1.6
	650	1.52	2.1	1.52
	800	1.72	2.15	1.52
	950	2.04	2.13	1.44
D (x=0.47)	as-deposited	1.12	2.41	1.7
	500	1.37	2.36	1.65
	800	1.8	2.48	1.5

C. Photoluminescence measurements

Photoluminescence experiments were performed for all the samples deposited on silicon substrates. The PL spectra have been reported in previous works for the samples of group A[27] and for samples of group C.[45] For this study, a synthesis of the results are presented in Fig. 7, where both intensity and energy of the PL maximum are represented as a function of the annealing temperature. The symbols correspond to the experimental data and the lines are drawn as a guide for the eyes. Whatever the chemical composition x of the films, a common evolution with the annealing temperature is observed. In a first step, the PL intensity increases until the annealing temperature T_{max} and then it decreases.

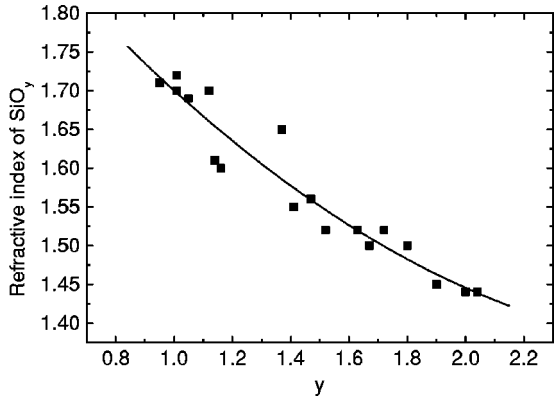

FIG. 6. Refractive index of the silicon oxide phase as a function of the stoichiometry of this phase. The curve is drawn as a guide for the eyes.

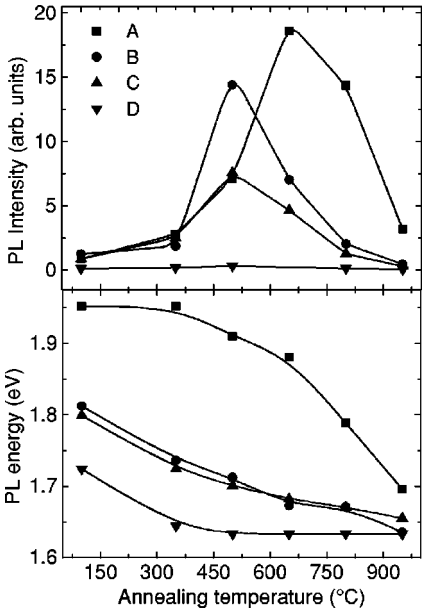

FIG. 7. Photoluminescence intensity and energy as a function of the annealing temperatures T_a for the samples of groups A, B, C, and D.

The PL intensity can be strongly improved by the annealing treatment. For example, it is multiplied by a factor around 20 for the sample A annealed at 650 °C. The PL is then very well visible to the naked eyes. For the samples annealed at 950 °C, the PL becomes very difficult to observe. For all the samples, the PL energy continuously decreases with increasing annealing temperature.

Alternative interpretations in literature are invoked to explain the origin of the PL phenomenon. The photoluminescence in such materials could be attributed to silicon oxide defect centers, interface states between the silicon clusters and the silicon oxide matrix, or to the quantum confinement effect. We believe a defect center's contribution to the PL phenomenon is very uncertain. Indeed the well known defect centers in silicon oxide materials involve a blue green radiative emission.[16] Furthermore, the PL energy is dependent on a particular defect and does not vary with annealing treatments. In this study, the PL is strongly modified by annealing treatments, which proves that determined defects are presumably not implicated in the PL emission. Because of the structural reorganization of the samples, the interface states could be modified during the thermal annealing treatments. In this hypothesis, the strong evolution of the PL could be correlated to the existence of interface states. However, in this case, there would exist a correlation between the stoichiometry of the silicon oxide matrix and the PL properties. The analysis of Figs. 4 and 7 shows that this correlation does not exist. The PL phenomenon can be explained by a quantum confinement effect in silicon grains embedded in the silicon oxide matrix. Due to the laser excitation, electron-hole pairs are created in the material and the recombination energy in the silicon grains is enlarged due to the size diminution. The strong PL intensity compared with that of bulk *a*-Si can be explained by the reduction of the nonradiative recombination channels caused by the carriers localization. Such an evolution of the PL intensity and energy with thermal annealing is in full agreement with the structural evolution of the materials. For as-deposited materials, the silicon grains are supposed to be very small and the PL energy is large. The structural study has shown that the volume fraction of silicon increases with annealing temperature. There is no direct evidence of the increase of the silicon clusters size, but it can be supposed that the silicon volume fraction is correlated to the increase of the silicon grains size and this could explain the decrease of the PL energy during annealing treatments. The evolution of the PL intensity is also well described by the quantum confinement model. Indeed, in the first stage of annealing, not only the silicon grains grow, which modifies the PL energy, but also new silicon grains are created, which improves the PL intensity. When the annealing temperature is greater than T_{max}, there is a coalescence phenomenon due to the clusters growth. The size of the silicon grains becomes too large to present the quantum confinement effect and the PL signal disappears.

In fact, the quantitative evolutions of both the PL energy and the PL intensity vary with the chemical composition of the film. T_{max} is equal to 650 °C for the $SiO_{0.95}$ samples of group A while it is equal to 500 °C for the samples of groups B, C, and D. This difference is explained by the fact that the formation of silicon clusters is more difficult in the high oxygen concentration film (group A). Due to the diffusion process, a higher annealing temperature is necessary to obtain the coalescence phenomenon of the silicon grains. For these films, until the annealing temperature is equal to 650 °C, the apparition of new clusters is dominant compared with the coalescence phenomenon. In the case of the coevaporated films the coalescence phenomenon appears at 500 °C because the silicon concentration is greater. Moreover, the value of the PL energy is an increasing function of x because it can be supposed that the average diameter increases with silicon concentration. In the case of high oxygen concentration films ($x=0.95$), the size of the silicon clusters is small. The confinement effect is greater and the PL energy is equal to 1.95 eV. For the other samples, the initial PL energy varies from 1.72 eV for $x=0.47$ to 1.82 eV for $x=0.75$. Furthermore the energy seems to converge for the high annealing temperatures to a common value equal to 1.6 eV. This limit tends to prove that there is a maximal size for the silicon clusters, above which the confinement effect disappears. For cluster sizes greater than the exciton Bohr radius, equal to 5 nm for silicon, the localization of the carriers disappears and the nonradiative recombinations are dominant. Theoretical works give an energy equal to 1.65 eV for silicon clusters with a diameter equal to 5 nm,[22,46] which is in agreement with this present work.

The exact dependence of the PL energy as a function of the cluster size is still a subject of controversy. It is admitted in the quantum confinement model that the energy decreases with the increasing grain size. As the precise size of the clusters is not known, the PL energy was represented in Fig. 8 as a function of the silicon volume fraction for all the samples. The curve is qualitatively a pertinent argument in favor of a quantum confinement effect because, whatever the average composition of the film and the annealing temperature, the value of the PL energy decreases with the increasing

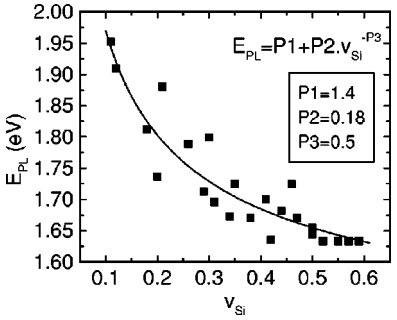

FIG. 8. Photoluminescence energy E_{PL} as a function of the silicon volume fraction v_{Si}. The parameters of the fitted curve are given on the figure.

silicon volume fraction. The fitted curve drawn in this figure is a power law with an exponent equal to 0.5. Considering the silicon volume fraction v_{Si} is proportional to r_{Si}^3, where r_{Si} is the radius of the silicon cluster, the PL energy is proportional to $r_{Si}^{-1.5}$, which is close to the $d^{-1.39}$ law given by Delerue *et al.*[20]

IV. CONCLUSION

Silicon oxide thin films were prepared by evaporation and coevaporation. The photoluminescence in the visible range was obtained for all the studied samples whatever their chemical composition. A structural study was performed to understand the origin of the PL phenomenon. The structural investigations have shown that the films are composed of amorphous silicon clusters embedded in a silicon oxide matrix and that a phase separation process appears during annealing treatments. Moreover optical measurements were performed and interpreted with the theory of the composite media. This analysis was in full agreement with the proposed structural model. Photoluminescence measurements indicated that both intensity and energy of emitted light are dependent on the chemical composition and annealing temperature. The correlation between structural and photoluminescence results strongly suggests that the origin of the photoluminescence is due to a quantum confinement effect of the electron-hole pairs in the amorphous silicon clusters. This work clearly shows that it is possible to obtain visible light emitting materials with silicon oxide films prepared by evaporation and that the crystallinity is not necessary to obtain radiative recombination in silicon clusters. It is also possible to control the PL energy by varying the chemical composition and the annealing temperature.

[1] L. T. Canham Appl. Phys. Lett. **57**, 1046 (1990).
[2] T. Shimizu-Iwayama, K. Fujita, S. Nakoa, K. Saitoh, T. Fujita, and N. Itoh, J. Appl. Phys. **75**, 7779 (1994).
[3] S. Guha, M. D. Pace, D. N. Dunn, and I. L. Singer, Appl. Phys. Lett. **70**, 1207 (1997).
[4] A. J. Kenyon, P. F. Trwoga, C. W. Pitt, and G. Rehm, J. Appl. Phys. **79**, 9291 (1996).
[5] E. Edelberg, S. Bergh, R. Naone, M. Hall, and S. Aydil, Appl. Phys. Lett. **68**, 1415 (1996).
[6] H. Z. Song, X. M. Bao, N. S. Li, and X. L. Wu, Appl. Phys. Lett. **72**, 356 (1998).
[7] D. J. Lockwood, Z. H. Lu, and J. M. Baribeau, Phys. Rev. Lett. **76**, 539 (1995).
[8] M. Ehbrecht, B. Hohn, F. Huisken, M. A. Laguna, and V. Paillard, Phys. Rev. B **56**, 6958 (1997).
[9] S. Schuppler, S. L. Friedman, M. A. Marcus, D. L. Adler, Y. H. Xie, F. M. Ross, Y. J. Chabal, T. D. Harris, L. E. Brus, W. L. Brown, E. E. Chaban, P. F. Szajowski, S. B. Christman, and P. H. Citrin, Phys. Rev. B **52**, 4910 (1995).
[10] M. S. Brandt, H. D. Fuchs, M. Stutzmann, J. Weber, and M. Cardona, Solid State Commun. **81**, 307 (1992).
[11] Y. D. Glinka, S. H. Lin, and Y. T. Chen, Appl. Phys. Lett. **75**, 778 (1999).
[12] J. Wang, L. Song, B. Zou, and M. A. El-Sayed, Phys. Rev. B **59**, 5026 (1999).
[13] S. M. Prokes, W. E. Carlos, S. Veprek, and Ch. Ossadnik, Phys. Rev. B **58**, 15632 (1998).
[14] A. G. Cullis, L. T. Canham, and P. D. J. Calcott, J. Appl. Phys. **82**, 909 (1997).
[15] D. P. Yu, Z. G. Bai, J. J. Wang, Y. H. Zou, W. Qian, J. S. Fu, H. Z. Zhang, Y. Ding, G. C. Xiong, L. P. You, J. Xu, and S. Q. Feng, Phys. Rev. B **59**, 2498 (1999).
[16] K. S. Min, K. V. Schlegov, C. M. Yang, H. A. Atwater, M. L. Brongersma, and A. Polman, Appl. Phys. Lett. **69**, 2033 (1996).
[17] S. T. Chou, J. H. Tsai, and B. C. Sheu, J. Appl. Phys. **83**, 5394 (1998).
[18] M. Rückschloss, B. Landkammer, and S. Veprek, Appl. Phys. Lett. **63**, 1474 (1993).
[19] H. Morisaki, F. W. Ping, H. Ono, and K. Yazawa, J. Appl. Phys. **70**, 1869 (1991).
[20] C. Delerue, G. Allan, and M. Lannoo, Phys. Rev. B **48**, 11024 (1993).
[21] N. A. Hill and B. Whaley, Phys. Rev. Lett. **75**, 1130 (1995).
[22] B. Delley and E. F. Steigmeier, Appl. Phys. Lett. **67**, 2370 (1995).
[23] A. D. Lan, B. X. Liu, and X. D. Bai, J. Appl. Phys. **82**, 5144 (1997).
[24] S. Charvet, R. Madelon, F. Gourbillau, and R. Rizk, J. Appl. Phys. **85**, 4032 (1999).
[25] M. J. Estes and G. Moddel, Phys. Rev. B **54**, 14633 (1996).
[26] G. Allan, C. Delerue, and M. Lannoo, Phys. Rev. Lett. **78**, 3161 (1997).
[27] H. Rinnert, H. Vergnat, G. Marchal, and A. Burneau, Appl. Phys. Lett. **72**, 3157 (1998).
[28] T. Inokuma, Y. Wakayama, T. Muramoto, R. Aoki, Y. Kurata, and S. Hasegawa, J. Appl. Phys. **83**, 2228 (1997).
[29] M. Zacharias, J. Bläsing, P. Veit, L. Tsybeskov, K. Hirschman, and P. M. Fauchet, Appl. Phys. Lett. **74**, 2614 (1999).
[30] M. A. Paesler, D. A. Anderson, E. C. Freeman, G. Moddel, and W. Paul, Phys. Rev. Lett. **41**, 1492 (1978).
[31] *The Physics of Hydrogenated Amorphous Silicon II*, edited by G. Lucovsky and J. D. Jaonnopoulos (Springer, Berlin, 1984), p. 325.
[32] G. Lucovsky, J. Yang, S. S. Chao, J. E. Tyler, and W. Czubatyj, Phys. Rev. B **28**, 3225 (1983).
[33] S. Y. Lin, J. Appl. Phys. **82**, 5976 (1997).
[34] H. Z. Song, X. M. Bao, N. S. Li, and X. L. Wu, Appl. Phys. Lett. **72**, 356 (1997).
[35] P. G. Pai, S. S. Chao, Y. Takagi, and G. Lucovsky, J. Vac. Sci. Technol. B **4**, 689 (1986).
[36] D. V. Tsu, G. Lucovsky, and B. N. Davidson, Phys. Rev. B **40**, 1795 (1989).
[37] M. Zacharias, D. Dimova-Malinovska, and M. Stutzmann, Philos. Mag. B **73**, 799 (1996).
[38] B. J. Hinds, F. Wang, D. M. Wolfe, C. L. Hinkle, and G. Lucovsky, J. Non-Cryst. Solids **227**, 507 (1998).
[39] K. Furukawa, Y. Liu, H. Nakashima, D. Gao, K. Uchino, K. Muraoka, and H. Tsuzuki, Appl. Phys. Lett. **72**, 725 (1997).
[40] F. Rochet, G. Dufour, H. Roulet, B. Pelloie, J. Perrière, E. Fogarassy, A. Slaoui, and M. Froment, Phys. Rev. B **37**, 6468 (1987).
[41] *Handbook of Optical Constants of Solids,* edited by E. D. Palik (Academic, New York, 1985), pp. 571, 765, and 749.
[42] J. L. Yeh and S. C. Lee, J. Appl. Phys. **79**, 656 (1996).
[43] K. Haga and H. Watanabe, Jpn. J. Appl. Phys., Part 1 **29**, 636 (1990).
[44] R. Swanepoel, J. Phys. E **16**, 1214 (1983).
[45] H. Rinnert, M. Vergnat, and G. Marchal, Mater. Sci. Eng., B **69–70**, 484 (2000).
[46] M. J. Estes and G. Moddel, Appl. Phys. Lett. **68**, 1814 (1996).